Honours Thesis Title

Samuel Moore
Supervisors: W/Prof Jim Williams, Prof Sergey Samarin
Honours Thesis submitted as part of the B.Sc. (Honours) degree
in the School of Physics, University of Western Australia

Date of submission: –/–/2012

Acknowledgments

I am extremely grateful for the support offered to me by many individuals during this project. There aren't many synonyms for "Thanks", so I'm afraid this section may be a little repetitive.

Thanks to my supervisors Prof Sergey Samarin and W/Prof Jim Williams for envisioning the project, and their invaluable support throughout the year. I would also like to thank staff members at CAMSP for assisting with the supervision of this project. In particular I am extremely grateful for the help and advice given by Dr Paul Gualiardo during the construction and testing of the Total Current Spectroscopy experiment.

Thanks to the Centre for Microscopy Characterisation and Analysis (CMCA) for producing the SEM images which proved a invaluable aid for discussing the structure of the metallic-black films. Thanks to Nikita Kostylev for helping me learn the art of operating the ellipsometer. Thanks to both Prof Mikhail Kostylev and Jeremy Hughes for lending me some samples for ellipsometric analysis. I would also like to endorse the team at J.A Woolam, who provided replacement pins for the ellipsometer alignment detector at no charge after one of the original pins became mysteriously damaged.

Congratulations to Jeremy Hughes who successfully predicted that the emission current of the electron gun was varying periodically less than a quarter of the way through the first period. Condolences to Alexander Mazur, whose theory that the vacuum chamber contained a pulsar proved unfounded.

Thanks to all my family and friends for their support and for continuing to put up with my slow descent into madness during the last 12 months.

Finally, perhaps as a result of the aforementioned madness, I would also like to thank the various pieces of equipment and inanimate objects which have been crucial to the success of this project. This includes the ellipsometer, the ADC/DAC box, my laptop computer "Cerberus", and the two ammeters upon which I relied upon so heavily. Rest in peace Keithly 610B. Your death was not in vain.

Abstract

Contents

Chapter 1

Introduction

So called metallic-black films are the result of deposition of metal elements at a relatively high pressure (of the order of 10^{-2} mbar). The films are named due to their high absorbance at visible wavelengths; they appear black to the naked eye. There is a remarkable contrast between such films and films deposited under low pressure (less than 10^{-6}mbar), which are typically highly reflective and brightly coloured.

This phenomenom has been known since the early 20th century, with the first papers on the subject published by Pfund in the 1930s [**?**], [**?**]. Pfund established the conditions for formation of metallic-blacks [**?**], and showed that the transmission spectrum of metallic black films is almost zero in visible wavelengths, but increases to a plateau in the far infrared [**?**]. More extensive research on the structural and optical properties of these films by Louis Harris and others during the 1940s and 1950s [**?**], [**?**], [**?**].

Harris et al. have produced experimental results of the transmission of metallic-black films from visible wavelengths to the far-infrared []. By modelling the film as a layer of metallic strands, acting as "condensors", Harris et al. arrived at an expression for the electron relaxation time of [element]-black [], leading to a a transmission spectrum in good agreement with experimental results.

Mckenzie has established that the presence of oxygen effects the optical and electrical properties of metallic-blacks [**?**].

More recently, it was shown that Au-black coatings increased the efficiency of thin film solar cells []. In this study, a simulation approximating an Au-black film as a layer of semi-spherical structures showed plasmonic behaviour which lead to an increase in electric field behind the film.

Metallic-black films have proven useful in applications requiring efficient absorption of light, including the. Recently there has been interest in artificial "blackening" of metal surfaces in ways which simplify the characterisation of the surfaces for prac-

tical applications.

Sondergaard et al. have produced metallic-black surfaces capable of suporting surface plasmon modes [**?**]. These films exhibit similar optical properties to the previously considered "evaporated" metallic-black surfaces.

This project will employ several techniques, including:Total Current Specroscopy; Ellipsometry and Optical Spectroscopy to investigate the difference between metallic films deposited at low pressure, and high pressure (metallic-blacks).

Chapter 2

Overview of Theory

Chapter 3

Experimental Techniques

3.1 Total Current Spectroscopy

In Total Current Spectroscopy experiments, a current of primary electrons I_1 is directed at a target surface. Upon interacting with the surface, the primary electron beam is split into two components; the transmitted current I, and the secondary electron current I_2. The current of secondary electrons includes all electrons emergent from the surface, regardless of origin. Generally I_2 includes components formed from elastically and inelastically scattered primary electrons, as well as electrons originating from bound states which have gained sufficient energy to leave the surface.

For any given mechanism behind the origin of an electron in I_2, there is an associated "threshold" primary electron energy which must be exceeded before the process can occur. As a result, measurement of changes in I_2 as a function of primary electron energy E_1 provides a very sensitive means to characterise properties of the sample under bombardment. The energy E_1 of primary electrons is controlled by adjustment of the potential U.

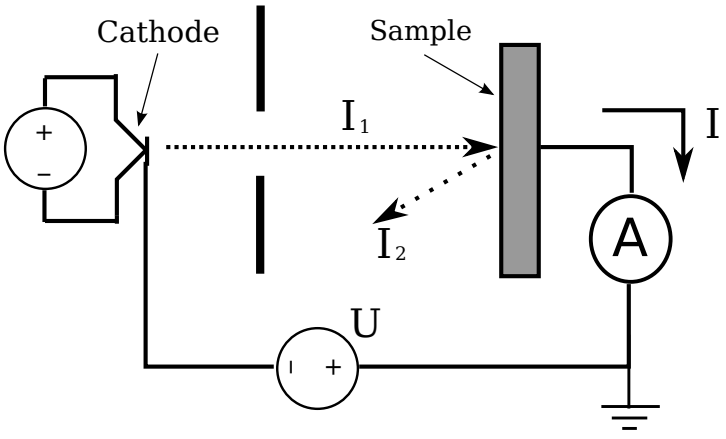

Figure 3.1: A simplified schematic of Total Current Spectroscopy Experiments

Figure **??** shows a simplified schematic for a Total Current Spectroscopy experiment [1]. When a current is passed through the cathode, electrons are thermionically emitted with a distribution in initial velocities. A series of electrodes (an electron gun) creates a potential which focuses the emitted electrons into a beam and accelerates them towards the target. The transmitted current I can be detected external to the vacuum chamber using a conventional DC ammeter[2].

The total current spectrum (TCS) is defined as:

$$S(E_1) = \frac{dI}{dE_1} = -\frac{dI_2}{dE_1}$$

This result assumes that the primary electron current I_1 is constant. Such an assumption is valid if the cathode has reached thermal equilibrium, and the potential due to the sample can be considered to have negligable effect on the focusing properties of the electron gun.

The experimental goal of Total Current Spectroscopy is the measurement of $S(E_1) \propto \frac{dI_2}{dE_1}$. More information on the experimental setup and techniques are presented in Appendix **??**. The remainder of this section will give an overview of concepts needed for relating $S(E_1)$ to properties of a sample.

Theory of Signal Formation in Total Current Spectroscopy Experiments

Here we will summarise the approach of Komolov [**?**] in constructing a theory relating $S(E_1)$ to scattering events within the target surface.

A single electron arriving at the sample has energy $E = eU + c$, where e is the electron charge, U is the potential applied between the cathode and sample, and c is a constant which includes the electron's energy relative to the sample when emitted. The minimum value for c is the contact potential of the cathode relative to the sample.

At the cathode, electrons are emitted with a distribution in energies about some mean value. A realistic model should take into account this distribution.

If the primary electrons are incident perpendicular to the surface, then we can write I as an integral over the whole distribution of energies:

$$I(E_1) = eA \int_0^\infty f(E - E_1) dE$$

where $f(E - E_1)$ is the distribution for an electron of energy E arriving at the

[1] For a more detailed description of the experimental setup, refer to Appendix **??**

[2] It is also possible to use lock-in amplifier techniques for noise reduction [**?**]. In this study, the DC ammeter has been used due to the relative simplicity of the measurement and control circuit.

surface. Generally $f(0)$ (ie: $E = E_1$) is the maximum of f.

TODO: Discuss angular distribution of incident electrons, due to focusing of electron gun?

To formulate a general expression for the secondary current, we introduce a cross section $\sigma(E)$, which gives the probability for a primary electron of energy E to give rise to a secondary electron (of any energy $E_2 <= E$).

Then the total current of secondary electrons is:

$$I_2(E_1) = eA \int_0^\infty f(E - E_1)\sigma(E)dE$$

Using $I = I_1 - I_2$, and $S(E_1) = \frac{dI}{dE_1}$, it is straight forward to arrive at a general expression for the total current spectrum [**?**]:

$$S(E_1) = eA \left\{ [1 - \sigma(0)]f(-E_1) + \int_0^\infty f(E - E_1)\frac{d\sigma(E_1)}{dE_1}dE \right\}$$

All E_1 dependence in the first term is due soley to the distribution of primary electrons. It is clear that this term is maximised when $E_1 = 0$ with respect to the sample; ie: the contact potential between the cathode and sample is zero.

The second term contains dependence upon $\frac{d\sigma(E_1)}{dE_1}$. As E_1 is increased past the threshold for a particular interaction, $\sigma(E_1)$ will undergo a sharp change. This corresponds to a narrow maxima or minima in the derivative $\frac{d\sigma(E_1)}{dE_1}$. A corresponding maxima or minima will appear in $S(E_1)$, centred about the threshold for the interaction. The convolution with the primary electron distribution $f(E - E_1)$ has the effect of broadening and lowering these peaks; in other words, the resolution of Total Current Spectroscopy is limited by the distribution of primary electrons.

The (unphysical) case of a mono-energetic beam is equivelant to setting $f(E - E_1) = \delta(E - E_1)$. In this case, the integrals in the expressions for I and I_2 collapse, and the resulting total current spectrum is:

$$S(E_1) = \frac{dI}{dE_1} = eA\frac{d}{dE_1}\left(1 - \sigma(E_1)\right) = eA\frac{d\sigma(E_1)}{dE_1}$$

3.2 Ellipsometry

Ellipsometry is an optical technique which measures the change in polarisation of light reflected from a surface. This change in polarisation can be related to properties of the surface; a common application of ellipsometry is determining the thickness of multilayered thin films.

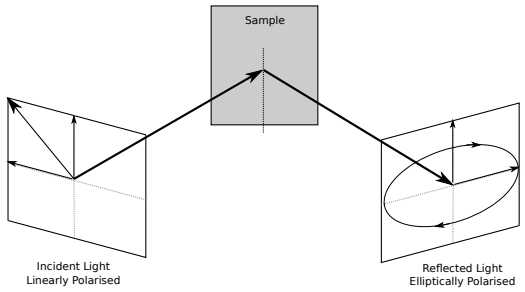

Figure 3.2: Diagram of Ellipsometry Measurements

As shown in figure **??**, linearly polarised light incident upon a surface is in general reflected as elliptically polarised light. Ellipsometers are designed to produce a known linear polarisation of light incident on a sample, and to record the polarisation of reflected light.

In the Jone's formalism, polarisation states may be represented by orthogonal electric field components E_p and E_s, which are polarised parallel and perpendicular to the plane of incidence respectively. The reflection of a light ray from the surface is described by the matrix equation:

$$\begin{bmatrix} E_{rp} \\ E_{rs} \end{bmatrix} = \begin{bmatrix} r_{pp} & r_{ps} \\ r_{sp} & r_{ss} \end{bmatrix} \begin{bmatrix} E_{ip} \\ E_{is} \end{bmatrix}$$

Where $\boldsymbol{E}_i$ and $\boldsymbol{E}_r$ are the incident and reflected rays. Each element of the 2×2 matrix r_{ij} is the reflection coefficient for i polarised light due to incident j polarised light; these values are generally complex to include the phase change.

Generalised Ellipsometry measures three ratios of r_{ij} values:

$$\rho_{pp} = \frac{r_{pp}}{r_{ss}} = \tan\psi_{pp} e^{-i\Delta_{pp}}$$
$$\rho_{ps} = \frac{r_{ps}}{r_{ss}} = \tan\psi_{ps} e^{-i\Delta_{ps}}$$
$$\rho_{sp} = \frac{r_{sp}}{r_{ss}} = \tan\psi_{sp} e^{-i\Delta_{sp}}$$

If the sample is isotropic, then $r_{ps} = r_{sp} = 0$. In this case, only the ratio $\frac{r_p}{r_s} = \frac{r_{pp}}{r_{ss}}$ must be measured:

$$\tan(\psi)e^{i\Delta} = \rho = \frac{r_p}{r_s} \tag{3.1}$$

The parameter ψ gives the angle by which ...., whilst Δ gives the phase difference between E_p and E_s components. The Jone's formalism is not sufficient to describe the response of samples which de-polarise the incident beam; the more general Stoke's formalism must be used for such cases [?] [?].

3.2.1 Variable Angle Spectroscopic Ellipsometry

Traditional ellipsometers were restricted to single angle and often single wavelength measurements []. With advances in computing technology in the 1970s,

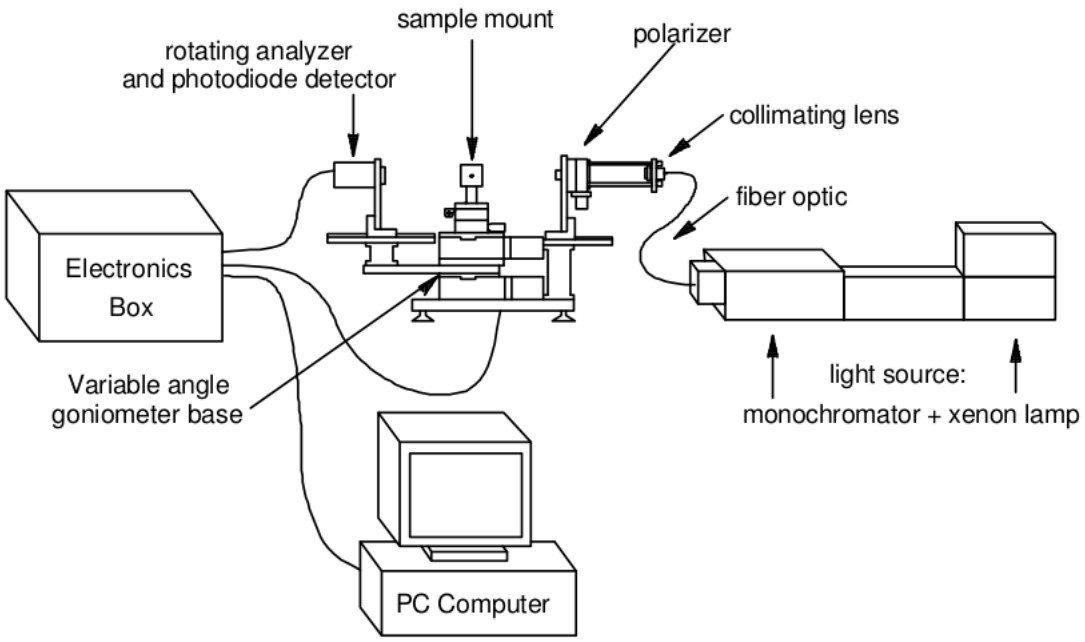

Figure 3.3: Block diagram of the VASE
(taken from *Overview of Variable Angle Spectroscopic Ellipsometry (VASE), Part I: Basic Theory and Typical Applications* [?])

3.3 Transmission Spectroscopy

3.4 Scanning Electron Microscopy

Chapter 4

Results and Discussion

4.1 Scanning Electron Microscopy

Nanostructured metal films prepared at low pressure are often approximated by an isotropic layer of spherical blobs upon the substrate, or even as a uniform layer with an "effective" thickness []. As the right image in Figure **??** shows, this is a good representation of the structure of such a film. In contrast, the metallic-black film is highly non-uniform; as a result, detailed characterisation of the properties of such a film is difficult.

4.2 Total Current Spectropy

4.3 Variable Angle Spectroscopy Ellipsometry

4.4 Optical Transmission Spectroscopy

Chapter 5

Conclusion

In conclusion, AAAAAAAAAAAAAAAAAAAAAAAAAAAAA

Electron Optics

There are two goals of electron optics as applied to total current spectroscopy (and other forms of electron scattering experiments): firstly, to produce the narrowest possible distribution $f(E - E_1)$ of primary electron energies at the sample, and secondly, to ensure that

The electron gun used for this study contains a total of ten electrodes, with six independently adjustable groups. Figure **??** illustrates a cross section of the gun, using colour coding to indicate groups of electrodes which are kept at the same potential.

The important electrode groups are, in order from left to right:

1. **Wenhalt Cylindar**

   The first electrode, which houses the cathode, providing a narrow apparture for electrons to exit. A positive potential (of the order of $10V$ applied to the Wenhalt causes electrons leaving the cathode to be accelerated into a narrow beam.

   It is difficult to control the focusing properties of the gun using the Wenhalt alone; the main purpose of the Wenhalt is to create a high current, narrow beam of electrons, which can be focused by the other electrodes in the gun. If the potential applied to the Wenhalt is too high, electrons will be drawn into its surface. If the Wenhalt potential is too low, then the

2. **Einzel Lens**

   The six central electrodes are an example of an Einzel lens, used for acceleration and focusing of the electron beam. The first and last pair of electrodes are held at a large positive potential, causing electrons to accelerate. A smaller potential (often negative, but not necessarily) applied to the central pair of electrodes has the effect of altering the angular dispersion of the beam.

3. **Deflection Plates**

   Unequal potentials applied to the deflection plates can be used to bend the direction of the electron beam. To ensure the accelerating potential seen by the

electrons is as uniform as possible, the deflection plates are biased at potentials of $\frac{V_d}{2} \pm V_a$, with V_d determined by the controlling power supply. When $V_d = 0$, the beam is undeflected.

4. **Final Electrode**

   The electron gun was originally designed for use in a Cathode Ray Oscilloscope (CRO). This electrode is held just in front of a flurescent screen, but is not electrically connected to the screen. When accellerated electrons strike the screen, they are

   In the total current spectroscopy experiments, this electrode is typically at a much higher potential than the surface under bombardment. As a result, low energy primary electrons may be deflected or even turned back towards the gun, rather than striking the surface. This effect can be exploited to narrow the energy distribution of primary electrons at the surface, but also has the effect of greatly reducing the current of primary electrons reaching the surface.

In preparation for Total Current Spectroscopy experiments, the effect of each of the controllable potentials was investigated by focusing the electron gun on its original flurescent screen. However, when repurposed for total current spectroscopy, the gun needed to be refocused several times (with changing sample holder design).

From **??**, it is apparent that the electron gun should be focused to achieve the maximum possible resolution by producing the narrowest possible primary energy distribution at the target. In addition, to increase the energy range (relative to the target), it

The gun was focused using an iterative process, by which each potential was altered in turn to maximise the current.

.1 A two dimensional electron gun simulation

The below figures **??** and **??** are the results of a simplistic electron gun simulation. The results of this simulation were not used to focus the actual electron gun; the images shown here are purely presented as a visual aid.

Figure 1: **2D Simulation of trajectories of electrons accelerated through an electron gun**

Figure 2: **2D Simulation of the electrostatic potential produced by the electron gun**

Electron Gun Control Circuit

The control circuit diagram for the electron gun is shown in Figure **??**. The wiring of the circuit, including resistors and potentiometers, was incoroprated into a single box, with external connections available for the power supplies, ammeters, electron gun, and sample holder. Both the components and operation of this circuit are straightforward; we will give a brief overview here for completeness.

- **Filament Heating** A constant current power supply is used to heat the filament. The inability to directly attach a wire to the filament leads to the requirement for biasing resistors in parallel with the filament. If the resistors are equal valued, assuming that each half of the filament has equal resistance, it is trivial to show that the potential of the emitting tip of the cathode is equal to that at the midpoint of the resistors.

  NOTE: I suspect the periodically changing emission current may be due to temperature dependence of the resistance of the **resistors***, since the current through the parallel circuit is constant, but not necessarily the filament if R is not constant. However, I have not had time to test this.*

- **Applied Potential** As discussed in Section **??**, the energy of electrons arriving at the sample is proportional to U (plus a constant). For this experiment, the power supply for setting U has been chosen to allow for serial control using a Digital to Analogue Convertor (DAC). Refer to Appendix **??** for more information.

- **Electrode Potentials** Seperate power supplies have been used for each independent electrode potential. The power supplies are biased to the cathode, rather than the sample; this ensures that changes in U do not effect the optics of the gun.

  - **Deflection Plates** The deflection plates are referenced to the accelerating electrodes (connections not shown). By using a dual gang potentiometer, with one electrode wired in the opposite direction to the other, the deflection plates will always be at $\frac{V_d}{2} \pm V_a$.

- **Current Measurement** Three current measurement points are available:
  - **Sample Current** This is the current measured during Total Current Spectroscopy experiments (see **??**). The ammeter used for this measurement provides an analogue output signal; Appendix **??** discusses the use of Analogue to Digital Conversion for automating the Total Current Spectroscopy experiments.
  - **Primary Electron Current** By applying Kirchoff's law, it can be seen that the sum of currents passing through a gun electrode or the sample is equal to the current flowing through this measurement point. This measurement point was used to verify that the primary current was constant, as assumed by Total Current Spectroscopy theory. Although some variation in primary electron current was observed, this occured over an extremely long timescale compared to the timescales involved with sample current measurement.
  - **Leak Current** The third measurement point includes electrons which travel through the accelerating electrodes or deflection plates. Knowledge of the current lost through electrodes before the surface was useful for optimising the current incident on the surface.

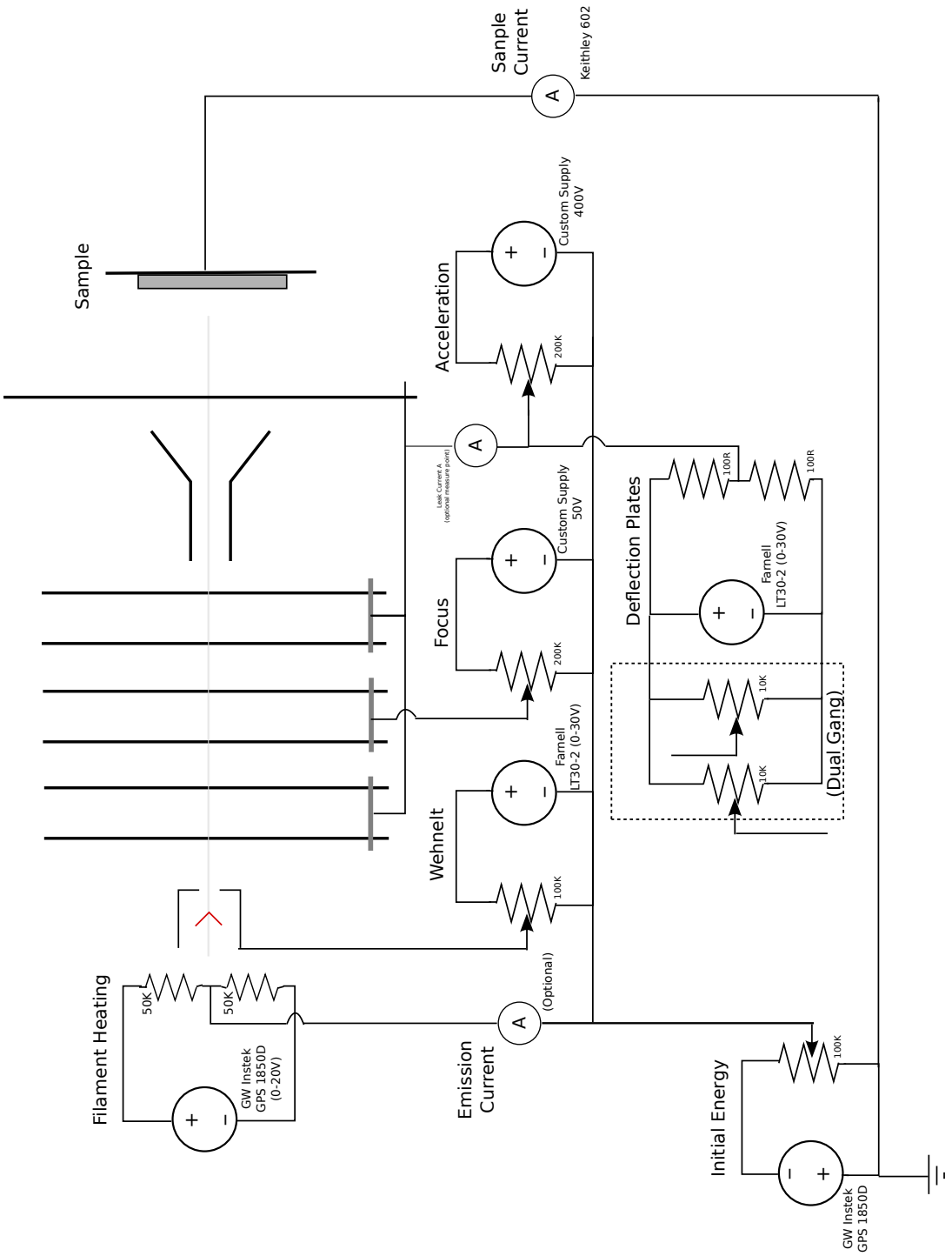
Sample
Sanple Current
Keithley 602
A
Custom Supply 400V
Acceleration
200K
Leak Current A (optional measure point)
Custom Supply 50V
Focus
200K
Farnell LT30-2 (0-30V)
Wehnelt
100K
Deflection Plates
100R
100R
Farnell LT30-2 (0-30V)
10K
10K
(Dual Gang)
Filament Heating
50K
50K
GW Instek GPS 1850D (0-20V)
Emission Current
(Optional)
Initial Energy
100K
GW Instek GPS 1850D

Figure 3: Circuit Diagram for Electron Gun Control